APPENDIX A

"Ultra-sensitive DNA Detection on Microarrays" by Jacak, *et al.*, Proc.Spie 5699 (2005) 442-449

Ultra–sensitive DNA detection on microarrays

Jaroslaw Jacak[1], Jan Hesse[*1], Clemens Hesch[1], Maria Kasper[2], Fritz Aberger[2], Annemarie Frischauf[2], Max Sonnleitner[3], Günter Freudenthaler[3], Stefan Howorka[3], and Gerhard J. Schütz[1]

[1]Biophysics Institute, Johannes Kepler University Linz, Altenberger Str.69, 4040 Linz, Austria;
[2]Division of Genomics, Department of Molecular Biology, University of Salzburg, Austria;
[3]Center for Biomedical Nanotechnology, Upper Austrian Research GmbH, Scharitzerstr.6-8, A-4020 Linz, Austria

ABSTRACT

Genomic research is nowadays based on high throughput analytical techniques. Microarray assays are commonly used to determine DNA content of heterogeneous mixtures up to full genome scale. For low amounts of sample material this method, however, requires time consuming and error prone PCR based amplification steps. Here, we present an assay with the ability to characterize the cDNA content of a low number of cells using ultra-sensitive fluorescence microscopy.

For detection, a newly developed chip reader was used. The instrument is based on a modified fluorescence microscope with single dye sensitivity. The highly sensitive CCD detector is operated in TDI mode, which allows avoiding overhead times for sample positioning and signal integration. This enabled the scanning of areas of $1x0.2cm^2$ within 50 seconds at a pixel size of 200nm. At this resolution, single dye molecules can be reliably detected with an average signal to background noise ratio of ~42.

For DNA hybridization experiments, oligonucleotides were covalently linked to a newly developed aldehyde surface. Subsequently, fluorescence labeled complementary oligonucleotides were hybridized at various concentrations. Down to femto-molar oligonucleotide concentrations, specific signals were detected. At 10fM concentration signals of individual specifically hybridized oligonucleotide molecules were resolvable. This assay provides the conceptual basis for expression profiling of low amounts of sample material without signal amplification.

Keywords: ultra-sensitive scanning, fluorescence microscopy, microarrays, oligonucleotides, single dye detection.

*jan.hesse@jku.at, phone: +43-732-2468-9288, http://www.biophysics.jku.at/bioph/staf/hesse/hesse.htm

1. INTRODUCTION

Microarray technology is a widely used approach for massively parallel detection of biological target molecules. It allows gaining insights into properties of cells or tissues through the determination of RNA and protein expression profiles. These profiles can be used to study the dependence of phenotypic aberrations on the expression of specific genes or proteins (*1*). Microarrays are presently applied to genotyping (*2*) and comparative hybridization studies of genomic DNA (*3*). However, when only minute amounts of sample material are available, unambiguous identification of aberrant genotypes still remains a difficult task. There, a limitation is set by the sensitivity of commercially available microarray platforms. Conventionally, this problem is circumvented by using PCR amplification methods to increase the amount of sample. It is known, however, that the efficiency of PCR amplification depends on DNA sequence and structure (*4*) and PCR can therefore cause statistically distorted outputs for heterogeneous DNA mixtures.

Recent advances in fluorescence detection techniques extended the range of sensitivity down to the level of single dye molecules (*5*) (*6*). For applying such devices in medical diagnostics, high throughput capabilities have to be achieved. We developed a novel fluorescence reader that has the capability for fast detection of single molecules on biochips (*7*). In the work presented here, we show the feasibility of this reader for DNA microarray analysis by hybridizing Cy5 labeled 60mer oligonucleotides (sense) to fully complementary oligonucleotides (antisense) covalently bound to a glass surface.

2. SETUP

The reader (figure 1) is based on a conventional epi-fluorescence microscope (Zeiss, Axiovert 200). For fluorescence excitation, 633nm and 647nm laser light from a dye and a Kr^+-ion (dye) laser (Coherent Innova 301), respectively, is used. To achieve a homogeneous excitation profile and an adjustable spot size, the shape of the laser beam is controlled using two cylindrical telescopes. Additionally, this configuration allows controlling the divergence of the laser beam (Köhler illumination). Adjustment of the incident angle of the laser at the surface of the sample is achieved by changing the angle of the incoming laser beam at the epi-port of the microscope. The excitation intensity was set to $0.135kW/cm^2$ at 647nm for the experiments on oligonucleotides and to $0.5kW/cm^2$ at 633nm for bilayer experiments. Fluorescence light is collected using a 100x oil immersion objective (Zeiss, α-Fluar, NA=1.45). Residual Rayleigh and Raman scattered light is effectively blocked using standard Cy3 and Cy5 filter sets (Chroma). Signals are detected on a back-illuminated NTE/CCD camera (Roper Scientific, QE≥85%). This camera uses an asymmetric CCD chip with C=1340pixels in serial and L=100pixels in parallel direction (pixel size: 20μm) and can be operated in time delayed integration (TDI) mode. For precise positioning, samples are mounted on a scanning stage (Märzhäuser, Scan IM 120x100) with 20nm minimum step size. The stage is equipped with an optical encoder system for closed loop sample positioning with ±100nm accuracy.

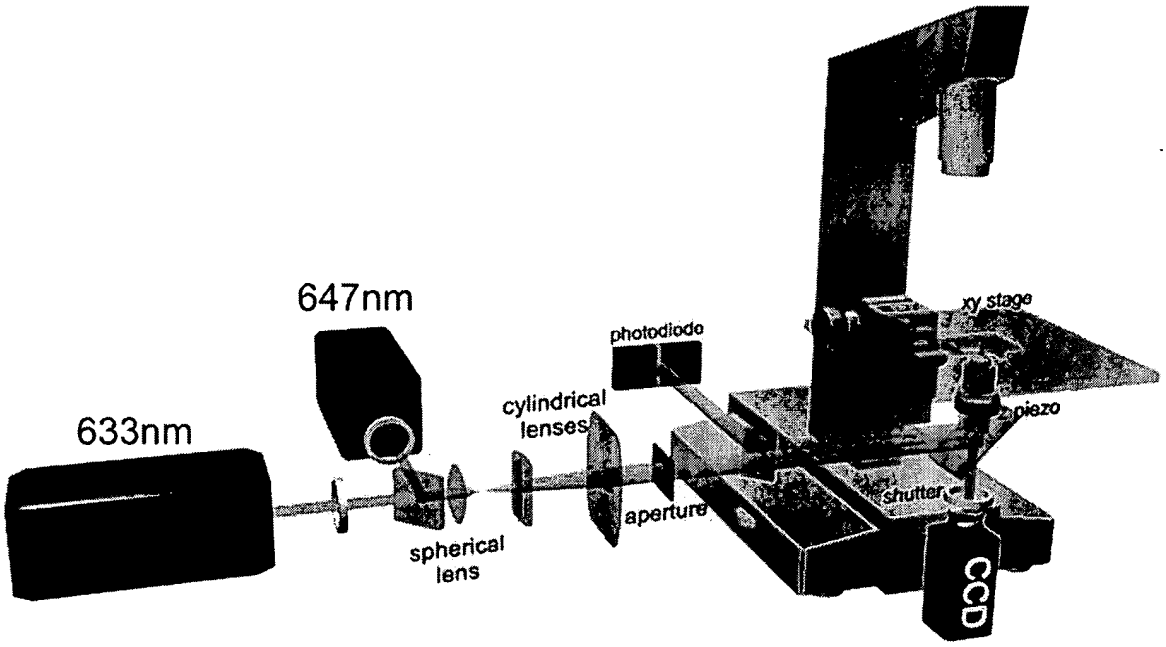

Figure 1 The setup is based on a conventional inverted epi–microscope (Zeiss, Axiovert 200). A dye and a Kr^+-ion laser emitting at 633nm and 647nm, respectively, are used for fluorescence excitation. Proper beam shaping is achieved using the combination of one spherical lens (f=19mm) and two cylindrical lenses (f=40mm and f=200mm). The sample is illuminated through a 100x objective and mounted on a xy–stage with 20nm step size. Fluorescence is collected using the same 100x objective and detected using a CCD camera (Roper Scientific). For automated maintenance of the focal position, the reflected excitation beam in TIR mode is detected on a 2–segment photodiode. The focus hold system uses the differential signal of this diode to control the position of the objective mounted on a z–piezo.

TDI mode detection has been developed for astronomy to acquire long swaths of moving objects, especially at low light levels (*8*). It requires the synchronization of the parallel register shift with the object motion, so that charge packets on the CCD pixels always correspond to the same image region as they move across the parallel register. Thereby, charge

accumulates and signal strength increases as the pixels approach the read-out register. Because of the continuous read out, TDI mode operation allows to acquire images larger than the actual chip size.
Synchronization of sample and image shift is achieved by running the camera as master, which provides trigger signals upon each line shift. This trigger is used to control the movement of the sample mounted on the xy-stage. Here, we use this imaging mode to achieve high signal to noise ratios when detecting single fluorescent molecules on areas in the range of square centimeters (*9*).
TDI mode imaging allows minimizing overhead times for time-consuming sample positioning with accuracies in the 100nm range. In contrast to conventional methods, TDI based scanning allows reaching the theoretical minimum for the scanning time of

$$T_{TDI} = \frac{A}{\delta^2} \cdot \left[t_{read-out} + \frac{t_{line-shift}}{C} \right] + \left[\frac{\sqrt{A}}{C\delta} \right] \cdot (LCt_{read-out} + Lt_{line-shift} + t_{positioning})$$

with A the area to be imaged, δ the pixel size in the object plane, $t_{read-out}$ the time to digitize each pixel, $t_{line-shift}$ the time to shift one line into the read-out register and $t_{positioning}$ additional terms accounting for positioning the stage; L and C the total number of lines and columns on the CCD chip, respectively.

The illumination time t_{ill} in TDI mode depends on the read out speed of the used camera and the excitation profile. The telescope allows independent adjustment of the widths and divergences of the laser beam in two perpendicular axes. An additional aperture in the beam path is used to fine-tune the size of the illuminated sample area to the size of the detection area and yields a homogeneous rectangular excitation spot with a size of 20µm x 200µm (corresponding to 100 x 1000pixels on the CCD chip at M=100). For quantitative imaging, residual inhomogeneities of the excitation profile have been corrected. The illumination time in this configuration is equal to the time required for reading one frame of the CCD $t_{ill} = L \cdot \left[C \cdot t_{read-out} + t_{line-shift} \right]$. For the camera used in this study, t_{ill} equals 100ms and the total recording time in TDI mode for a 1x0.02cm stripe is 50s. For the gaussian excitation profile used in the bilayer experiments, the illumination time can be calculated using $\hat{t}_{ill} = \sqrt{2\pi}\sigma \cdot \left[C \cdot t_{read-out} + t_{line-shift} \right]$ (*7*) and is equal to 53ms.

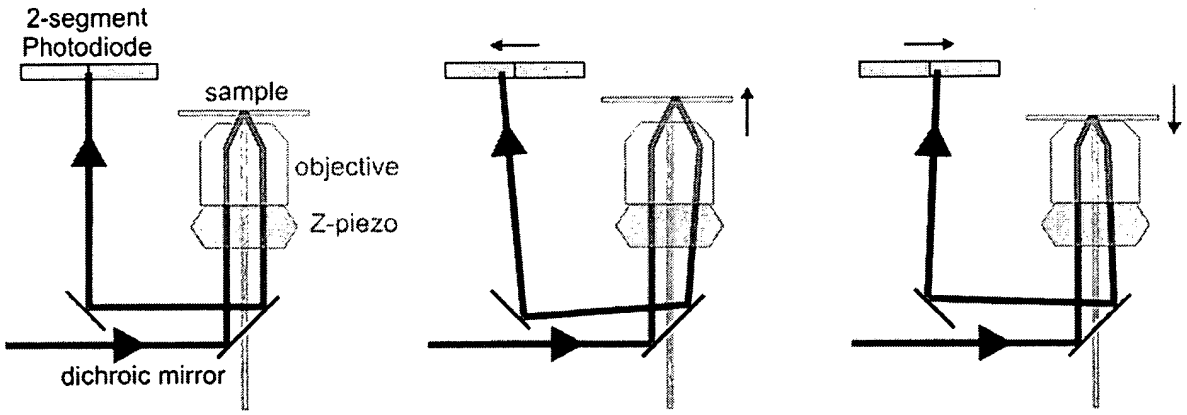

Figure 2 Operation principle of the focus hold system. Upon defocusing of the sample, the reflected laser beam changes its position on the 2-segment photodiode. The differential signal of the two diodes is a sensitive measure for the focal position and is used to control a feed-back loop to the z-piezo.

To image arbitrary sample sizes, the setup allows scanning of neighboring stripes and images in the range of square centimeters can be obtained. To ensure proper focusing over such large images, an automatic focus-hold system has been set up (*10, 11*). For this purpose, the laser is adjusted slightly out of the optical axis of the objective which results in a non-perpendicular incident angle at the sample surface. The step in the refraction index from glass to buffer causes the laser light to be partially reflected at the sample surface. The reflected light is spatially separated from the incident

beam (see figure 2) and can be guided onto a 2-segment photodiode using a simple mirror. Upon changes in the distance between objective and sample surface, the angle of the reflected laser beam changes (figure 2). This deflection is detected using a 2-segment photodiode (Hamamatsu) whose differential signal is used as input into a PID controller operated in feedback loop; the output of this controller is connected to a piezo driven focusing system (Physik Instrumente).

3. SAMPLE PREPARATION

3.1. Supported DPPC bilayers containing DPPE-Cy5

For a proof of principle experiment, the device was used to image a supported lipid bilayer on a glass cover-slip, containing trace amounts of fluorescent labeled lipid. The bilayer was formed by vesicle fusion (*12*). Briefly, 2.5mg/ml dipalmitoyl-phosphatidycholine (DPPC, Avanti Polar Lipids) containing a molar fraction of 10^{-8} Cy5-labelled dipalmitoyl-phosphatidylethanolamine (Cy5-DPPE (*13*)) were sonicated in phosphate buffered saline (PBS). Glass cover-slips were incubated with 10µl of the resulting vesicle solution for 30minutes at room temperature. Prior to the fluorescence read out, the vesicle solution was diluted with 1ml pure PBS to remove remaining vesicles from the glass surface. The formed bilayer was imaged in TDI mode with an illumination time of 53ms. At room temperature, DPPC lipid forms a bilayer in gel phase; the matrix is characterized by a lateral diffusion constant of $D_{lat} \sim 10^{-12} cm^2/s$ (*14*), which allows to treat individual Cy5-DPPE molecules as immobilized on the length and time scale of the experiment.

3.2. Oligonucleotides on coverslips

For hybridization experiments, custom made aldehyde coated cover-slips (Upper Austrian Research GmbH) were used. Amino-reactive 60-mer oligonucleotides specific for Xenopus Xag-2 RNA (VBC-Genomics) were bound to the chip surface as capture sequences. For higher coupling efficiency, the capture sequence contained a short 12 carbon long crosslinker between the oligonucleotides and the amino-group. After 1 day incubation period, the unbound oligonucleotides were removed by extensive washing with blocking buffer containing 10µM sodium cyanoborohydride for reducing the Schiff bases and forming a stable covalent bond between chip surface and oligonucleotides.

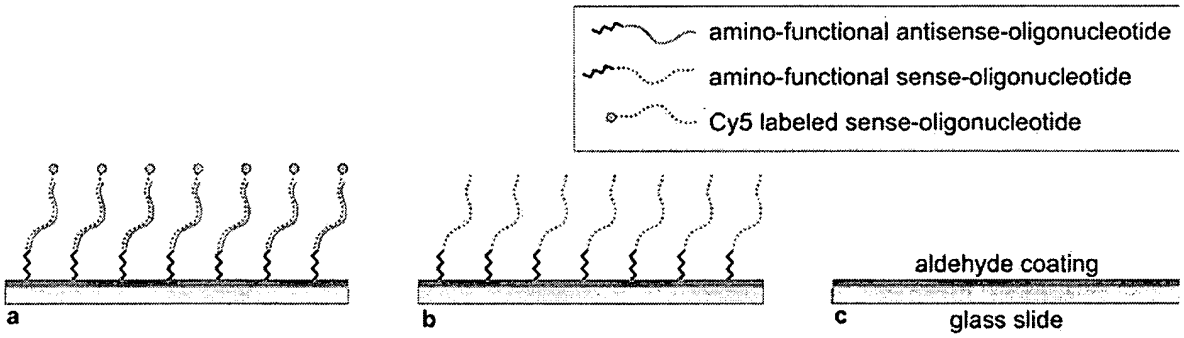

Figure 3 Sketch visualizing the chip surfaces used for hybridization experiments with labeled sense-oligonucleotides. **(a)** Aldehyde coated glass slide, surface functionalized with antisense-oligonucleotides and specifically hybridized labeled sense-oligonucleotides. **(b)** Surface functionalized with sense-oligonucleotides. **(c)** Not functionalized glass slides with aldehyde coating after blocking procedure. **(a-b)** The 12 carbon long crosslinker (solid black line) increases the coupling efficiency of the capture probes to the aldehyde coating.

For specific hybridization, the antisense functionalized surfaces were incubated with Cy5 labeled complementary 60mer sense-oligonucleotides. Hybridization was performed for one hour at room temperature in 4xSSC buffer containing 10fM Cy5 labeled sense-oligonucleotides and 0,1% SDS (Sodiumdodecylsulfat). The chips were subsequently washed with various concentrations of SSC (Saline-Sodium Citrat) buffer containing SDS. Finally, samples were covered with 0,1 SSC buffer for microscopy. To achieve comparable results, these conditions were kept constant throughout the experiments presented in this paper. Negative control experiments were performed under identical conditions using glass slides functionalized with non-complementary sense oligonucleotides or left not functionalized.

4. RESULTS

4.1. Single dyes in lipid bilayers

Fluorescence images from lipid bilayers were recorded in TDI mode with scan lengths in the millimeter range. No significant defocusing was observed over the whole scan length. Images appear homogeneous and contain randomly distributed fluorescent peaks, as expected from previous measurements on similar systems (*15, 16*).

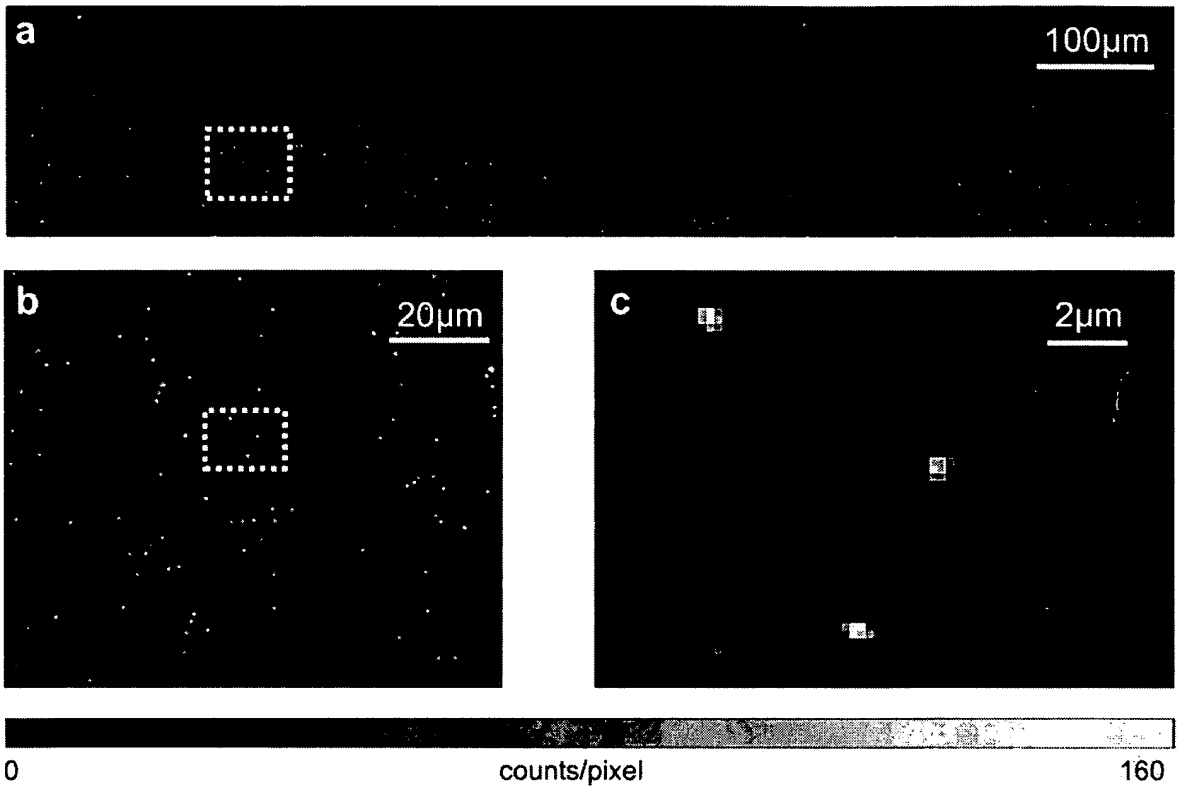

Figure 4 (a) 1 × 0.2mm^2 area of a DPPC bilayer containing a molar fraction of 10^{-8} Cy5–labelled DPPE molecules. The image has been recorded in TDI mode within 50s. Fluorescent peaks, corresponding to Cy5 labelled DPPE molecules, are randomly distributed over the whole area. No defocusing is observed over the 1mm scan. **(b)** and **(c)** are details of **(a)** and **(b)**, respectively, showing single molecule signals as bright diffraction limited spots. All images have been corrected for residual variations in the excitation profile using the intensity profile of the exciting laser spot.

The surface density was found to be approximately 1.4 Cy5-DPPE molecules per 100µm^2. Assuming a mean area of 48Å^2 per DPPC molecule (*17*), this values compares well with the theoretical prediction of 2.1 molecules/100µm^2. Signals of individual fluorescent peaks were analyzed by fitting an elliptical 2-dimensional Gaussian function (*18*), which accounts for the point spread function of the microscope and the TDI mode specific image-distortion in scanning direction (*19*). Analysis of 1350 diffraction limited fluorescent peaks yielded an average $FWHM_1 = 510\text{nm}$ in scanning direction, and $FWHM_2 = 450\text{nm}$ in the perpendicular direction. While the latter value compares well with the previously characterized width of the point spread function in the focal plane $FWHM_{PSF} = 470\text{nm}$ (*20*), the width in scanning direction shows the expected increase of ~13% compared to the perpendicular axis.

The experiments on lipid bilayers were performed using a dye laser emitting at 633nm and the illumination time was set to 53ms. The fit with an elliptical Gaussian function yields a median intensity of ~812counts per individual fluorescent peak. Taking into account the excitation intensity of ~0.5kW/cm^2 and the illumination time of 53ms, this value is in good agreement with previous results on this fluorophore containing bilayer system (*13*). The high signal amplitude enables easy discrimination of individual fluorescent peaks against the background. The background noise of 10conts rms corresponds to 22counts per diffraction limited spot and yields a signal to background noise ratio of ~37. This high value enables unambiguous detection of basically all fluorophores on the glass slide.

4.2. Oligonucleotides on coverslips

Samples with hybridized cDNA oligonucleotides were scanned in TDI mode as described above. All samples showed randomly distributed fluorescent signals (figure 5), indicating binding of Cy5 labeled oligonucleotides on the surface of the chip. The image in figure 5a shows a 4800μm^2 image of a antisense-functionalized glass slide with specifically bound sense oligonucleotides. Bright fluorescent peaks with an average density of 6 molecules per 100μm^2 are clearly visible. Unspecific binding of labeled oligonucleotides to the surface was quantified on samples containing non-complementary sense oligonucleotides (figure 5b) and unfunctionalized surfaces (figure 5c); the same hybridization procedure was performed for all experiments. The surface density on the sense-functionalized chips decreased by a factor ~5 (~1.1 molecules per 100μm^2) compared to the functionalized sample areas indicating cross-hybridization between labeled sense oligonucleotides and sense nucleotides on the chip surface. On unfunctionalized chips the surface density further decreased to ~0.1 molecules per 100μm^2 which shows the good anti-adsorptive properties of the used surfaces.

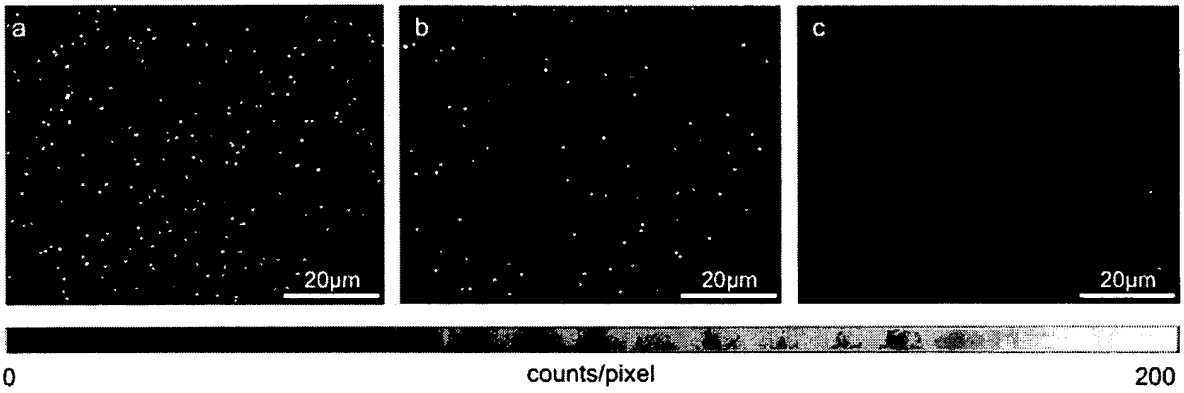

Figure 5 80μm x 60μm images of **(a)** specifically functionalized (antisense), **(b)** unspecifically functionalized (sense) and **(c)** not functionalized glass slides after hybridization with 10fM Cy5 labeled oligonucleotides. Fluorescent signals of single labeled molecules are clearly visible as diffraction limited bright spots. **(a)** Specific hybridization yields a surface density of 6 molecules/100μm^2. **(b)** Unspecific signal caused by cross-hybridization of labeled sense oligonucleotides with sense nucleotides on the chip surface yields a surface density of ~1.1 molecules/100μm^2. **(c)** Unspecific adsorption to not functionalized chip surfaces results in a weak background signal of ~0.1 molecules/100μm^2.

For detailed analysis, the fluorescent signals were fitted with an elliptical Gaussian function. Analyzing the peaks width perpendicular to and in scanning direction showed the expected peak broadening of ~14%. Both values, $FWHM_1 = 514\text{nm}$ in scanning direction and $FWHM_2 = 450\text{nm}$ perpendicular to it, are near the diffraction limit of $FWHM_{PSF} = 470\text{nm}$.

A median intensity of ~1188counts was obtained for diffraction limited peaks. Taking into account the different illumination parameter, this value compares well with data recorded on individual fluorescent lipids (figure 4). For this comparison, we calculated the fluorescence intensity normalized by illumination time and excitation intensity, yielding 48cnts (53cnts) for lipids (oligonucleotides). Considering the low background noise of 16 counts rms, corresponding to 28counts per diffraction limited spot, this yields a signal to noise ratio of ~42 for single labeled oligonucleotides (figure 6).

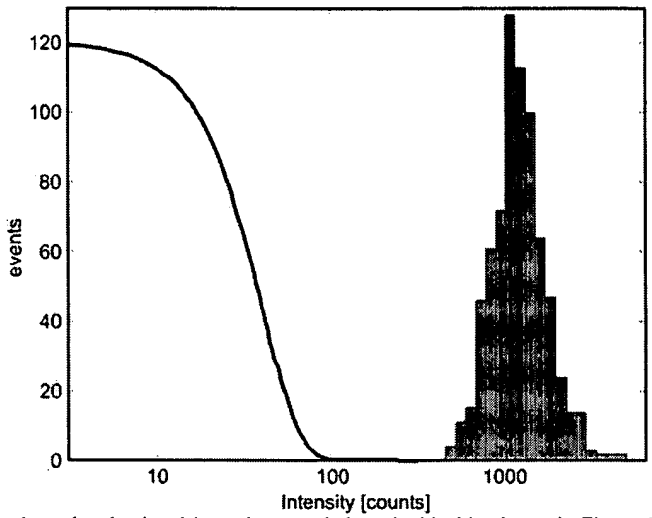

Figure 6 Histogram of the single-molecule signal intensity recorded on the biochip shown in Figure 5, plotted in logarithmic scale. The median signal of 1188counts clearly exceeds the background noise of 28counts per diffraction limited spot, yielding a mean signal to background noise ratio of ~42. This allows one to unambiguously detect basically all dye molecules on the glass slide. To improve visibility, distribution of the background signal has been plotted as a probability density function.

5. CONCLUSIONS

The single molecule sensitivity of the presented microscope has been shown on DPPC bilayer containing trace amounts of Cy5-labeled DPPE molecules. At a molar ratio of $1:10^8$ individual Cy5-DPPE molecules have been detected in the DPPC matrix at a signal to noise ratio of ~37, which allows detecting basically all labeled molecules located at the sample surface. The width of the diffraction limited peaks remained constant over the whole scan length of 1mm, demonstrating the proper function of the focus hold system. Furthermore, the slight peak broadening in scanning direction of ~13% indicates a good synchronization of sample movement and CCD camera read-out.

We demonstrated the applicability of this setup for the ultra-sensitive chip-based DNA detection using specific oligonucleotide hybridization as a test system. Down to incubation concentrations of 10fM, specific signals from individual oligonucleotides hybridized to their complementary sequence on the chip have been detected. Even at the low labeling stoichiometry of 1 dye molecule per oligonucleotide, we achieved a signal to background noise ratio of 42, which allows unambiguously counting all oligonucleotides on the chip.

The presented setup is a promising tool for detection of trace amounts of sample cDNA without the need for prior amplification steps like e.g. PCR, which are time consuming and might cause quantification errors. Applying the presented technology to DNA microarrays has the potential for expression profiling of minute amounts of sample down to the level of single molecules.

ACKNOWLEDGEMENTS

This study was supported by the GEN-AU program of the Austrian Federal Ministry of Education, Science and Culture, by the Austrian Research Funds (project number P15057), and by the state of Upper Austria.

REFERENCES

1. R. L. Strausberg, *J Pathol* **195**, 31 (2001).
2. J. Huang *et al.*, *Hum Genomics* **1**, 287 (May, 2004).
3. C. Brennan *et al.*, *Cancer Research* **64**, 4744 (2004).
4. G. L. Mutter, K. A. Boynton, *Nucleic Acids Res* **23**, 1411 (Apr 25, 1995).
5. S. Weiss, *Science* **283**, 1676 (Mar 12, 1999).
6. W. E. Moerner, M. Orrit, *Science* **283**, 1670 (1999).
7. J. Hesse *et al.*, *Analytical Chemistry* **76**, 5960 (2004).
8. J. T. McGraw, J. R. P. Angel, T. A. Sargent, in *Applications of Digital Image Processing to Astronomy* D. A. Eliot, Ed. (SPIE, Bellingham, 1980), vol. 264, pp. 20.
9. H. Schindler, in *PCT/AT99/00257*. (Schindler, H., international patent, 2000).
10. E. H. Hellen, D. Axelrod, *Review of Scientific Instruments* **61**, 3722 (1990).
11. M. Sonnleitner. (Austria, 2004).
12. E. Kalb, S. Frey, L. K. Tamm, *Biochim Biophys Acta* **1103**, 307 (Jan 31, 1992).
13. G. J. Schutz, G. Kada, V. P. Pastushenko, H. Schindler, *Embo J* **19**, 892 (2000).
14. L. K. Tamm, H. M. McConnell, *Biophys J* **47**, 105 (Jan, 1985).
15. G. S. Harms, M. Sonnleitner, G. J. Schutz, H. J. Gruber, T. Schmidt, *Biophys J* **77**, 2864 (1999).
16. G. J. Schutz, H. Schindler, T. Schmidt, *Biophys J* **73**, 1073 (1997).
17. W. Sun *et al.*, *Physical Review. E. Statistical Physics, Plasmas, Fluids, and Related Interdisciplinary Topics* **49**, 4665 (May, 1994).
18. T. Schmidt, G. J. Schutz, W. Baumgartner, H. J. Gruber, H. Schindler, *Proc Natl Acad Sci U S A* **93**, 2926 (1996).
19. B. K. Gibson, P. Hickson, *Mon. Not. R. astr. Soc* **258**, 543 (1992).
20. G. J. Schutz *et al.*, *Single Mol.* **1**, 25 (10 Apr 2000, 2000).